

Communication

Ball Milling-Assisted Synthesis of Ultrasmall Ruthenium Phosphide for Efficient Hydrogen Evolution Reaction

Xiaofei Liu ¹, Yanglong Guo ¹, Wangcheng Zhan ^{1,*} and Tian (Leo) Jin ^{2,*}

¹ Key Laboratory for Advanced Materials and Research Institute of Industrial Catalysis, School of Chemistry and Molecular Engineering, East China University of Science and Technology, Shanghai 200237, China; lilooliu@hotmail.com (X.L.); ylguo@ecust.edu.cn (Y.G.)

² Department of Applied Chemistry, School of Science, MOE Key Laboratory for Nonequilibrium Synthesis and Modulation of Condensed Matter (Xi'an Jiaotong University), Xi'an Key Laboratory of Sustainable Energy Materials Chemistry and State Key Laboratory for Mechanical Behavior of Materials, Xi'an Jiaotong University, Xi'an 710049, China

* Correspondence: zhanwc@ecust.edu.cn (W.Z.); tianjin.ecust@gmail.com (T.(L.)J.)

Received: 16 February 2019; Accepted: 1 March 2019; Published: 5 March 2019



Abstract: The development of scalable hydrogen production technology to produce hydrogen economically and in an environmentally friendly way is particularly important. The hydrogen evolution reaction (HER) is a clean, renewable, and potentially cost-effective pathway to produce hydrogen, but it requires the use of a favorable electrocatalyst which can generate hydrogen with minimal overpotential for practical applications. Up to now, ruthenium phosphide Ru₂P has been considered as a high-performance electrocatalyst for the HER. However, a tedious post-treatment method as well as large consumption of solvents in conventional solution-based synthesis still limits the scalable production of Ru₂P electrocatalysts in practical applications. In this study, we report a facile and cost-effective strategy to controllably synthesize uniform ultrasmall Ru₂P nanoparticles embedded in carbon for highly efficient HER. The key to our success lies in the use of a solid-state ball milling-assisted technique, which overcomes the drawbacks of the complicated post-treatment procedure and large solvent consumption compared with solution-based synthesis. The obtained electrocatalyst exhibits excellent Pt-like HER performance with a small overpotential of 36 mV at current density of 10 mA cm⁻² in 1 M KOH, providing new opportunities for the fabrication of highly efficient HER electrocatalysts in real-world applications.

Keywords: mechanochemistry; hydrogen evolution; electrocatalysts; ruthenium phosphide

1. Introduction

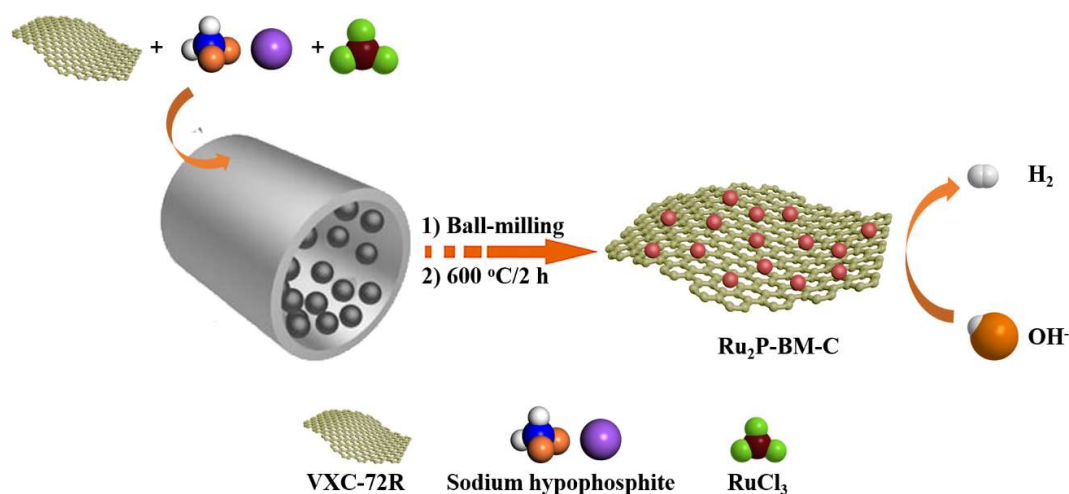
Renewable hydrogen energy, an ideal substitute for nonrenewable fossil fuels, has attracted much attention due to its zero emissions of greenhouse gases [1,2]. Therefore, the development of scalable hydrogen production technology to produce hydrogen economically and in environmentally friendly ways is particularly important. Among them, electrochemical water splitting is a new method for hydrogen production, which presents a clean, renewable, and potentially cost-effective pathway to produce hydrogen [3–5]. As a vital step of electrochemical water splitting on the cathode, the hydrogen evolution reaction (HER) always demands the use of a favorable electrocatalyst which can generate hydrogen with minimal overpotential for practical applications [6–8]. Up to now, precious platinum (Pt)-based catalysts have been widely acknowledged as unbeatable HER electrocatalysts due to their high current density and low Tafel slope [9–11]. However, their widespread utility is limited by natural scarcity. Therefore, research into novel types of HER catalysts with both high activity and low price is highly important.

Recently, ruthenium (Ru)-based catalysts have gradually emerged as a new type of promising HER electrocatalysts with high intrinsic catalytic activity, which are comparable to the commercial Pt-based catalysts [12–14]. Despite Ru being a precious transition metal belonging to the Pt group, the cost of Ru is only ca. 4% of the cost of Pt per unit mass [15]. Therefore, many efforts have been made to develop rationally designed Ru electrocatalysts with both high intrinsic HER performance and low cost. Inspired by the efficient metal phosphides catalysts used in the hydrodesulfurization (HDS) reaction, precious ruthenium phosphides such as RuP, RuP₂, and Ru₂P were well explored as high-performance electrocatalysts for the HER owing to their similarity in catalytic mechanisms [16–21]. For example, Liu et al. synthesized Ru₂P nanoparticle-decorated P/N-doped carbon nanofibers on carbon cloth involving electrochemical polymerization and subsequent metal impregnation [16]. Li et al. reported the example of Ru₂P nanoparticles supported on reduced graphene oxide nanosheets via a solution-based hydrothermal synthesis [20]. The moderate Gibbs free energy of hydrogen adsorption on the Ru₂P surface based on density function theory (DFT) calculations endows Ru₂P nanoparticles with excellent HER electrocatalytic performance. Until now, conventional solution-based synthesis was necessary for fabricating Ru₂P nanoparticles. However, the tedious post-treatment method as well as large consumption of solvents still limits the scalable production of Ru₂P electrocatalysts in practical applications. Therefore, developing a novel, facile, and environmental-friendly methodology for preparing high-performance Ru₂P electrocatalysts is of great significance.

In this study, we report a facile and cost-effective strategy to controllably synthesize uniform ultrasmall Ru₂P nanoparticles embedded in carbon for highly efficient HER. The key to our success lies in the use of a solid-state ball milling-assisted technique, which overcomes the drawbacks of complicated post-treatment procedure and large solvent consumption compared with solution-based synthesis. To the best of our knowledge, solid-state synthesis of Ru₂P nanoparticles has never been reported so far. More importantly, the obtained electrocatalyst exhibits excellent Pt-like HER performance with a small overpotential of 36 mV at a current density of 10 mA cm⁻² in 1 M KOH, providing new opportunities for the fabrication of highly efficient HER electrocatalysts in real application.

2. Results and Discussion

As shown in Scheme 1, we successfully fabricated Ru₂P nanoparticles embedded in carbon (Ru₂P-BM-C) via a simple solid-state ball milling-assisted technique [22]. To be specific, a mixture of ruthenium chloride, sodium hypophosphite, and commercial carbon black (VXC-72R, Cabot) were first milled in a planetary ball mill for 2 h. Subsequently, the resultant composite was further thermally treated under nitrogen atmosphere at 600 °C for 2 h (detailed synthetic information can be found in the experimental section).



Scheme 1. The synthesis route of Ru₂P nanoparticles embedded in carbon (Ru₂P-BM-C) via a facile ball milling-assisted method.

The structural features of as-prepared Ru₂P-BM-C were first determined by a representative X-ray diffraction (XRD) pattern. As illustrated in Figure 1, the characteristic diffraction peaks of Ru₂P-BM-C can be well indexed to a typical orthorhombic phase of ruthenium phosphide (Ru₂P, JCPDS No. 65-2382) [21]. Meanwhile, the broad diffraction peak centered at ca. 25° is assigned to commercial carbon black [23]. The contents of Ru and P in Ru₂P-BM-C were determined to be 5.1 and 0.81 wt%, respectively, as determined by inductively coupled plasma-mass spectrometry (ICP-MS), indicating a nearly 1.93:1 atomic ratio for Ru/P. In addition, the bulk morphology and distribution of Ru₂P in carbon matrix was further demonstrated by transmission electron microscopy (TEM). As shown in Figure 2a,b, a highly uniform dispersion of Ru₂P ultrasmall nanoparticles was observed, with an average size of ca. 5 nm. In addition, high-resolution transmission electron microscopy (HRTEM) of one grain oriented along the [112] zone axis is also shown in Figure 2c. The corresponding d-spacing is measured to be 2.36 Å, which matches very well with the result from XRD (Figure 1).

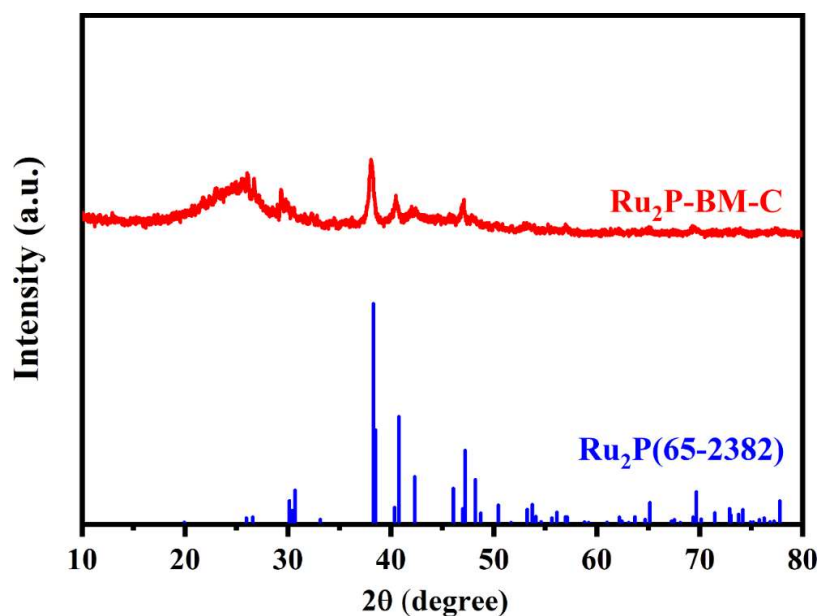


Figure 1. XRD pattern of Ru₂P-BM-C.

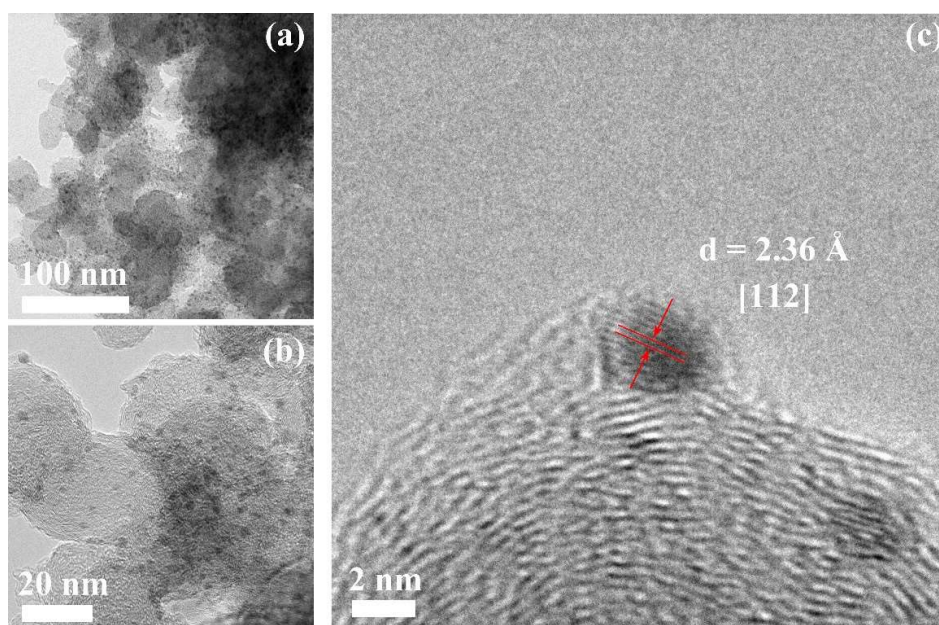


Figure 2. (a,b) TEM images and (c) HRTEM image of Ru₂P-BM-C.

To further probe the surface chemistry of Ru₂P-BM-C, X-ray photoelectron spectroscopy (XPS) was performed to analyze the surface chemical state of Ru₂P-BM-C. In the P 2p spectrum (Figure 3a), the peaks at 130.0 and 130.7 eV are attributed to Ru-P bonding. Meanwhile, the peak at 134.0 eV can be assigned to P-O signal, possibly from the oxidized P species under air [24]. For the Ru 3d spectrum (Figure 3b), subpeaks at 280.5 and 285.0 eV are consistent with the binding energies of Ru 3d_{5/2} and Ru 3d_{3/2} of Ru₂P [25,26], respectively, while the subpeak at 285.6 eV is associated with the C=O bond [27]. These results are consistent with the above XRD and HRTEM analysis, further confirming the successful formation of Ru₂P in carbon matrix.

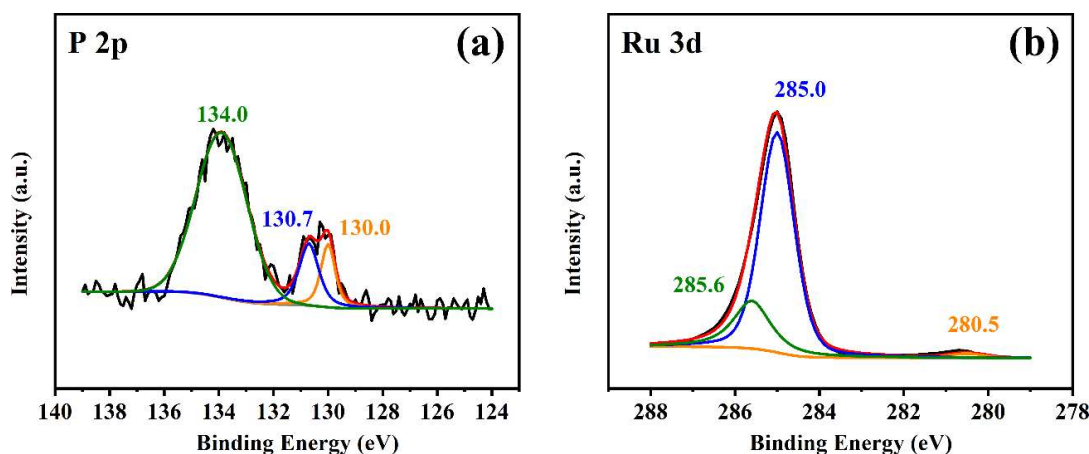


Figure 3. XPS spectra of P 2p (a) and Ru 3d (b) of Ru₂P-BM-C.

To evaluate the HER performance of Ru₂P-BM-C, we first studied the HER activity of Ru₂P-BM-C in N₂-saturated 1 M KOH. The sample was loaded on a polished glassy carbon (GC) electrode using a standard three-electrode cell. An Ag/AgCl electrode and a graphite rod were utilized as the reference and counter electrodes, respectively. Linear sweep voltammetry (LSV) measurements with a sweep rate of 5 mV s⁻¹ were performed to determine the HER activity of the sample and all polarization curves were corrected with iR-compensation. The overpotential to deliver 10 mA cm⁻² current density, a metric related to solar water-splitting devices, was then carefully measured to compare the HER activity for various electrocatalysts. As illustrated in Figure 4a, Ru₂P-BM-C presented a very small HER overpotential of 36 mV at a current density of 10 mA cm⁻² in 1 M KOH, which was very close to benchmark Pt/C (31 mV@10 mA cm⁻²), and obviously outperformed many previously reported Ru-based HER electrocatalysts such as Ru₂P nanoparticle-decorated P/N dual-doped carbon nanofibers on carbon cloth (Ru₂P@PNC/CC-900, 50 mV@10 mA cm⁻²) [16], Ru₂P nanoparticles (54 mV@10 mA cm⁻²) [21], carbon-encapsulated ruthenium diphosphide nanoparticle (RuP₂@NPC, 52 mV@10 mA cm⁻²) [19], RuP_x nanoparticles encapsulated in uniform N,P-codoped hollow carbon nanospheres (RuP_x@NPC, 74 mV@10 mA cm⁻²) [28], ruthenium incorporated cobalt phosphide nanocubes (Ru-CoP, 51 mV@10 mA cm⁻²) [29], and Ru nanodendrites composed of ultrathin fcc/hcp nanoblades (RuCu NDs, 43 mV@10 mA cm⁻²) [30], indicating the outstanding catalytic activity of Ru₂P-BM-C in alkaline electrolyte.

To get a better understanding of HER kinetics using Ru₂P-BM-C the corresponding Tafel plots of Ru₂P-BM-C and commercial Pt/C were investigated in 1 M KOH. Remarkably, Ru₂P-BM-C exhibits a low Tafel slope of 59 mV decade⁻¹ (Figure 4b), which is comparable to the value for the Pt/C catalyst (53 mV decade⁻¹). This reveals that the HER mechanism of our catalyst follows Volmer–Heyrovsky reaction where an initial proton adsorption is the rate-determining step [31]. Furthermore, the HER stability of Ru₂P-BM-C was also evaluated by cycling the Ru₂P-BM-C continuously for 2000 cyclic voltammetry (CV) cycles. The resultant LSV curve after 2000 cycles exhibited almost no difference compared with the initial one (Figure 4c), indicating robust stability of Ru₂P-BM-C under alkaline condition. The excellent long-term durability was also corroborated by TEM analysis. As shown

in Figure 5a,b, no obvious morphological change can be observed for Ru₂P nanoparticles after 2000 cycles, further confirming the high stability of Ru₂P-BM-C. Previous studies indicated that carbon-encapsulated electrocatalysts could significantly promote durability for HER, which may also contribute to the high stability of Ru₂P-BM-C [32–34].

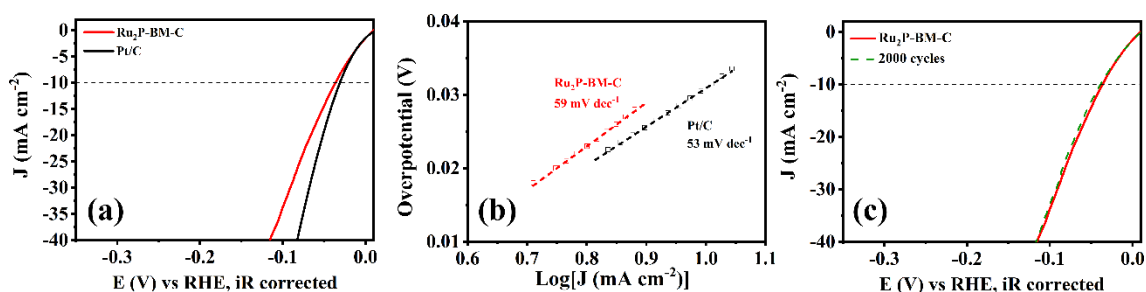


Figure 4. (a) Hydrogen evolution reaction (HER) polarization curves of Ru₂P-BM-C and benchmark Pt/C, respectively. (b) Tafel plots of corresponding Ru₂P-BM-C and Pt/C. (c) Polarization curves of the Ru₂P-BM-C catalyst decorated on a GC electrode before and after 2000 CV cycles. All tests were performed in 1 M KOH.

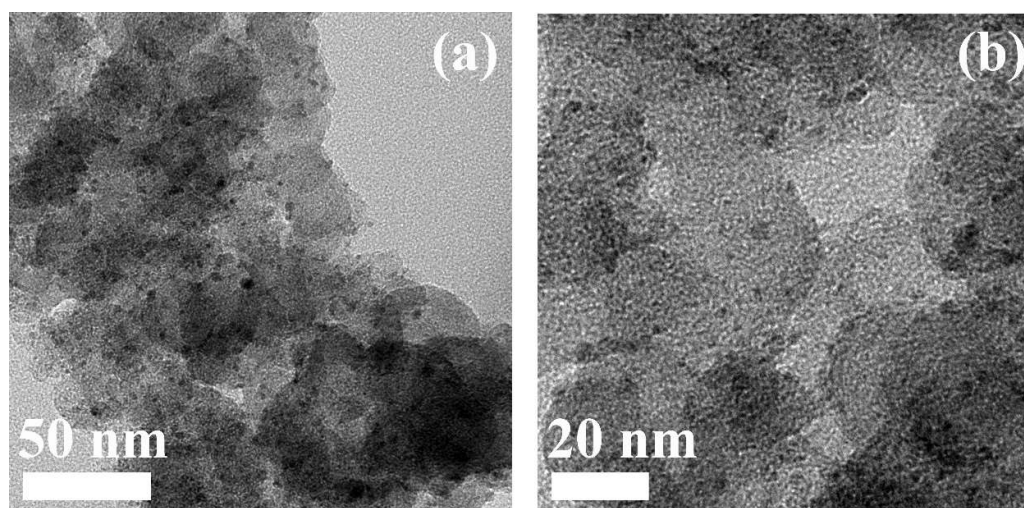


Figure 5. (a,b) TEM images of Ru₂P-BM-C after 2000 CV cycles.

3. Materials and Methods

3.1. Catalyst Preparation

In a typical synthesis, ruthenium chloride (24 mg, Aladdin, Shanghai, China) and sodium hypophosphite (500 mg, Aladdin, Shanghai, China) were mixed with commercial carbon black (100 mg, VXC-72R, Cabot, Kingchemical, Shanghai, China). The mixture was transferred to a commercially available PTFE ball mill jar (~20 mL) with twenty PTFE balls (6 mm in diameter). The reactor was placed in a high energy planetary ball mill (Changsha Deco Equipment Co., Ltd., Changsha, China, Model DECO-PBM-H-0.4L) and milled at 600 rpm for 2 h. After ball milling, the resulting product was pyrolyzed at 600 °C (heating rate: 5 K min⁻¹) for 2 h under an inert N₂ atmosphere. The resultant catalyst was washed and denoted as Ru₂P-BM-C.

3.2. Material Characterization

X-ray diffraction (XRD) was performed on a Bruker D8 ADVANCE diffractometer (Karlsruhe, Germany) using Cu-K α radiation with a 2 θ range of 10 to 80°. The morphology of the sample was investigated by using a JEOL JEM-F200 high-resolution transmission electron microscopy (Tokyo, Japan). X-ray photoelectron spectroscopic (XPS) measurement was performed on a Thermo Fisher

ESCALAB Xi+ spectrometer (Waltham, MA, USA) equipped with an Al-K α X-ray source. The contents of Ru and P were determined by inductively coupled plasma-mass spectrometry (ICP-MS, NexION 350D, PerkinElmer, Waltham, MA, USA).

3.3. Electrochemical Test

A CHI 650E electrochemical workstation (Shanghai, China) was used to measure the electrocatalytic activities towards HER. One molar KOH was utilized as the electrolyte. All experiments were conducted in a standard three-electrode electrochemical cell consisting of a glassy carbon as the working electrode substrate, a graphite rod as the counter electrode, and an Ag|AgCl (3.5 M KCl) electrode as the reference electrode. The potential measured against Ag|AgCl was further converted to the potential versus the reversible hydrogen electrode (RHE). iR-compensation was made to compensate for the voltage drop between the reference and working electrodes, which was measured by a single-point high-frequency impedance measurement. To fabricate the working electrode, 2 mg of each catalyst sample and 50 μ L of 5 wt% Nafion solution (D520, Alfa Aesar, Shanghai, China) were dispersed in 1 mL of water/ethanol solution (3:1 *v/v*) under mild sonication for at least 40 min to form a homogeneous ink. Thereafter, 12 μ L of the catalyst ink was dropped onto a mirror polished glassy carbon electrode with 3 mm in diameter and dried at ambient conditions. The loading amount of was calculated to be ~ 0.34 mg cm^{-2} . The benchmark Pt/C catalyst (20 wt% Pt, JM) was also prepared with equal loading. For HER tests, the electrolyte was saturated with argon for at least 30 min and continuous cyclic voltammetry sweeps were operated to make pretreatment. Linear scan voltammetry (LSV) was performed at a scan rate of 5 mV s^{-1} . To prevent formation of bubbles, magnetic stirring with a stir bar with the rotation rate of 800 rpm was employed for the LSV.

4. Conclusions

In summary, we developed a facile solid-state synthesis to prepare highly efficient HER catalysts with ultrasmall Ru₂P embedded in a carbon matrix. The key to our success lies in the use of a facile high-energy ball milling-assisted technique. As a result, the as-prepared Ru₂P-BM-C exhibits impressive HER activity with a small overpotential of 36 mV at the current density of 10 mA cm^{-2} in 1 M KOH, which exceeds that of many previously reported Ru-based electrocatalysts. Moreover, Ru₂P-BM-C also displays excellent electrochemical stability in alkaline electrolyte, with no activity loss after 2000 continuously CV cycles. Therefore, the well-designed Ru₂P-BM-C acts as a promising candidate for HER catalysts in real application.

Author Contributions: T.(L.)J. and W.Z. conceived the idea. X.L. designed the experiments and carried out most of the material synthesis and characterization. X.L., T.(L.)J., and Y.G. contributed to the experimental setup. X.L. and T.(L.)J. participated in the material synthesis and characterization. X.L. and T.(L.)J. cowrote the paper. All authors commented on the manuscript. T.(L.)J. supervised all experimental design, tests, and analysis.

Funding: This research was funded by the National Key Research and Development Program of China (2016YFC0204300), the National Natural Science Foundation of China (21577034), the Science and Technology Commission of Shanghai Municipality (16ZR1407900), Fundamental Research Funds for the Central Universities (222201717003), and the China Postdoctoral Science Foundation (2018M640970).

Acknowledgments: We thank the Instrument Analysis Center of Xi'an Jiaotong University for their support in characterization assistance.

Conflicts of Interest: The authors declare no conflict of interest.

References

1. Sivula, K.; Van de Krol, R. Semiconducting materials for photoelectrochemical energy conversion. *Nat. Rev. Mater.* **2016**, *1*, 15010. [[CrossRef](#)]
2. Cox, K.E.; Williamson, K.D. *Hydrogen: Its Technology and Implication: Production Technology*; CRC Press: Boca Raton, FL, USA, 2018; p. 4.

- Cao, L.; Luo, Q.; Liu, W.; Lin, Y.; Liu, X.; Cao, Y.; Zhang, W.; Wu, Y.; Yang, J.; Yao, T.; et al. Identification of single-atom active sites in carbon-based cobalt catalysts during electrocatalytic hydrogen evolution. *Nat. Catal.* **2019**, *2*, 134–141. [[CrossRef](#)]
- Zheng, Y.R.; Wu, P.; Gao, M.R.; Zhang, X.L.; Gao, F.Y.; Ju, H.X.; Wu, R.; Gao, Q.; You, R.; Huang, W.X.; et al. Doping-induced structural phase transition in cobalt diselenide enables enhanced hydrogen evolution catalysis. *Nat. Commun.* **2018**, *9*, 2533. [[CrossRef](#)] [[PubMed](#)]
- Dinh, C.T.; Jain, A.; de Arquer, F.P.G.; De Luna, P.; Li, J.; Wang, N.; Zheng, X.; Cai, J.; Gregory, B.Z.; Voznyy, O.; et al. Multi-site electrocatalysts for hydrogen evolution in neutral media by destabilization of water molecules. *Nat. Energy* **2019**, *4*, 107–114. [[CrossRef](#)]
- Wang, X.S.; Zhu, Y.H.; Vasileff, A.; Jiao, Y.; Chen, S.M.; Song, L.; Zheng, B.; Zheng, Y.; Qiao, S.Z. Strain Effect in Bimetallic Electrocatalysts in the Hydrogen Evolution Reaction. *ACS Energy Lett.* **2018**, *3*, 1198–1204. [[CrossRef](#)]
- Kagkoura, A.; Tzanidis, I.; Dracopoulos, V.; Tagmatarchis, N.; Tasis, D. Template synthesis of defect-rich MoS₂-based assemblies as electrocatalytic platforms for hydrogen evolution reaction. *Chem. Commun.* **2019**, *55*, 2078–2081. [[CrossRef](#)] [[PubMed](#)]
- Zheng, Y.; Jiao, Y.; Vasileff, A.; Qiao, S.Z. The Hydrogen Evolution Reaction in Alkaline Solution: From Theory, Single Crystal Models, to Practical Electrocatalysts. *Angew. Chem. Int. Ed.* **2018**, *57*, 7568–7579. [[CrossRef](#)] [[PubMed](#)]
- Li, T.F.; Liu, J.J.; Song, Y.; Wang, F. Photochemical Solid-Phase Synthesis of Platinum Single Atoms on Nitrogen-Doped Carbon with High Loading as Bifunctional Catalysts for Hydrogen Evolution and Oxygen Reduction Reactions. *ACS Catal.* **2018**, *8*, 8450–8458. [[CrossRef](#)]
- Xiang, Z.P.; Deng, H.Q.; Peljo, P.; Fu, Z.Y.; Wang, S.L.; Mandler, D.; Sun, G.Q.; Liang, Z.X. Electrochemical Dynamics of a Single Platinum Nanoparticle Collision Event for the Hydrogen Evolution Reaction. *Angew. Chem. Int. Ed.* **2018**, *57*, 3464–3468. [[CrossRef](#)] [[PubMed](#)]
- Li, K.; Li, Y.; Wang, Y.M.; Ge, J.J.; Liu, C.P.; Xing, W. Enhanced electrocatalytic performance for the hydrogen evolution reaction through surface enrichment of platinum nanoclusters alloying with ruthenium in situ embedded in carbon. *Energy Environ. Sci.* **2018**, *11*, 1232–1239. [[CrossRef](#)]
- Nong, S.Y.; Dong, W.J.; Yin, J.W.; Dong, B.W.; Lu, Y.; Yuan, X.T.; Wang, X.; Bu, K.J.; Chen, M.Y.; Jiang, S.D.; et al. Well-Dispersed Ruthenium in Mesoporous Crystal TiO₂ as an Advanced Electrocatalyst for Hydrogen Evolution Reaction. *J. Am. Chem. Soc.* **2018**, *140*, 5719–5727. [[CrossRef](#)] [[PubMed](#)]
- Li, Y.T.; Zhang, L.A.; Qin, Y.; Chu, F.Q.; Kong, Y.; Tao, Y.X.; Li, Y.X.; Bu, Y.F.; Ding, D.; Liu, M.L. Crystallinity Dependence of Ruthenium Nanocatalyst toward Hydrogen Evolution Reaction. *ACS Catal.* **2018**, *8*, 5714–5720. [[CrossRef](#)]
- Wang, Z.L.; Sun, K.J.; Henzie, J.; Hao, X.F.; Li, C.L.; Takei, T.; Kang, Y.-M.; Yamauchi, Y. Spatially Confined Assembly of Monodisperse Ruthenium Nanoclusters in a Hierarchically Ordered Carbon Electrode for Efficient Hydrogen Evolution. *Angew. Chem. Int. Ed.* **2018**, *57*, 5848–5852. [[CrossRef](#)] [[PubMed](#)]
- Su, J.W.; Yang, Y.; Xia, G.L.; Chen, J.T.; Jiang, P.; Chen, Q.W. Ruthenium-cobalt nanoalloys encapsulated in nitrogen-doped graphene as active electrocatalysts for producing hydrogen in alkaline media. *Nat. Commun.* **2017**, *8*, 14969. [[CrossRef](#)] [[PubMed](#)]
- Liu, T.T.; Feng, B.M.; Wu, X.J.; Niu, Y.L.; Hu, W.H.; Li, C.M. Ru₂P Nanoparticle Decorated P/N-Doped Carbon Nanofibers on Carbon Cloth as a Robust Hierarchical Electrocatalyst with Platinum-Comparable Activity toward Hydrogen Evolution. *ACS Appl. Energy Mater.* **2018**, *1*, 3143–3150. [[CrossRef](#)]
- Chang, Q.B.; Ma, J.W.; Zhu, Y.Z.; Li, Z.; Xu, D.Y.; Duan, X.Z.; Peng, W.C.; Li, Y.; Zhang, G.L.; Zhang, F.B.; et al. Controllable Synthesis of Ruthenium Phosphides (RuP and RuP₂) for pH-Universal Hydrogen Evolution Reaction. *ACS Sustain. Chem. Eng.* **2018**, *6*, 6388–6394. [[CrossRef](#)]
- Yu, J.; Guo, Y.N.; She, S.X.; Miao, S.S.; Ni, M.; Zhou, W.; Liu, M.L.; Shao, Z.P. Bigger is Surprisingly Better: Agglomerates of Larger RuP Nanoparticles Outperform Benchmark Pt Nanocatalysts for the Hydrogen Evolution Reaction. *Adv. Mater.* **2018**, *30*, 1800047. [[CrossRef](#)] [[PubMed](#)]
- Pu, Z.H.; Amiin, I.S.; Kou, Z.K.; Li, W.Q.; Mu, S.C. RuP₂-Based Catalysts with Platinum-like Activity and Higher Durability for the Hydrogen Evolution Reaction at All pH Values. *Angew. Chem. Int. Ed.* **2017**, *56*, 11559–11564. [[CrossRef](#)] [[PubMed](#)]

20. Liu, T.T.; Wang, S.; Zhang, Q.J.; Chen, L.; Hu, W.H.; Li, C.M. Ultrasmall Ru₂P nanoparticles on graphene: A highly efficient hydrogen evolution reaction electrocatalyst in both acidic and alkaline media. *Chem. Commun.* **2018**, *54*, 3343–3346. [[CrossRef](#)] [[PubMed](#)]
21. Wang, Y.; Liu, Z.; Liu, H.; Suen, N.-T.; Yu, X.; Feng, L.G. Electrochemical Hydrogen Evolution Reaction Efficiently Catalyzed by Ru₂P Nanoparticles. *ChemSusChem* **2018**, *11*, 2724–2729. [[CrossRef](#)] [[PubMed](#)]
22. Jin, T.; Sang, X.H.; Unocic, R.R.; Kinch, R.T.; Liu, X.F.; Hu, J.; Liu, H.L.; Dai, S. Mechanochemical-Assisted Synthesis of High-Entropy Metal Nitride via a Soft Urea Strategy. *Adv. Mater.* **2018**, *30*, 1707512. [[CrossRef](#)] [[PubMed](#)]
23. Su, Y.H.; Jiang, H.L.; Zhu, Y.H.; Yang, X.L.; Shen, J.H.; Zou, W.J.; Chen, J.D.; Li, C.Z. Enriched graphitic N-doped carbon-supported Fe₃O₄ nanoparticles as efficient electrocatalysts for oxygen reduction reaction. *J. Mater. Chem. A* **2014**, *2*, 7281–7287. [[CrossRef](#)]
24. Kibsgaard, J.; Jaramillo, T.F. Molybdenum Phosphosulfide: An Active, Acid-Stable, Earth-Abundant Catalyst for the Hydrogen Evolution Reaction. *Angew. Chem. Int. Ed.* **2014**, *53*, 14433–14437. [[CrossRef](#)] [[PubMed](#)]
25. Morgan, D.J. Resolving ruthenium: XPS studies of common ruthenium materials. *Surf. Interface Anal.* **2015**, *47*, 1072–1079. [[CrossRef](#)]
26. Srivastava, V. Functionalized Hydrotalcite Tethered Ruthenium Catalyst for Carbon Sequestration Reaction. *Catal. Lett.* **2018**, *148*, 1879–1892. [[CrossRef](#)]
27. Niu, Y.; Huang, X.; Hu, W. Fe₃C nanoparticle decorated Fe/N doped graphene for efficient oxygen reduction reaction electrocatalysis. *J. Power Sources* **2016**, *332*, 305–311. [[CrossRef](#)]
28. Chi, J.Q.; Gao, W.K.; Lin, J.H.; Dong, B.; Yan, K.L.; Qin, J.F.; Liu, B.; Chai, Y.M.; Liu, C.G. Hydrogen Evolution Activity of Ruthenium Phosphides Encapsulated in Nitrogen- and Phosphorous-Codoped Hollow Carbon Nanospheres. *ChemSusChem* **2018**, *11*, 743–752. [[CrossRef](#)] [[PubMed](#)]
29. Yan, Y.; Huang, J.; Wang, X.; Gao, T.; Zhang, Y.; Yao, T.; Song, B. Ruthenium Incorporated Cobalt Phosphide Nanocubes Derived From a Prussian Blue Analog for Enhanced Hydrogen Evolution. *Front. Chem.* **2018**, *6*, 521. [[CrossRef](#)] [[PubMed](#)]
30. Gao, K.; Wang, Y.; Wang, Z.W.; Zhu, Z.H.; Wang, J.L.; Luo, Z.M.; Zhang, C.; Huang, X.; Zhang, H.; Huang, W. Ru nanodendrites composed of ultrathin fcc/hcp nanoblades for the hydrogen evolution reaction in alkaline solutions. *Chem. Commun.* **2018**, *54*, 4613–4616. [[CrossRef](#)] [[PubMed](#)]
31. Jiang, H.L.; Zhu, Y.H.; Su, Y.H.; Yao, Y.F.; Liu, Y.Y.; Yang, X.L.; Li, C.Z. Highly dual-doped multilayer nanoporous graphene: Efficient metal-free electrocatalysts for the hydrogen evolution reaction. *J. Mater. Chem. A* **2015**, *3*, 12642–12645. [[CrossRef](#)]
32. Deng, J.; Ren, P.J.; Deng, D.H.; Yu, L.; Yang, F.; Bao, X.H. Highly active and durable non-precious-metal catalysts encapsulated in carbon nanotubes for hydrogen evolution reaction. *Energy Environ. Sci.* **2014**, *7*, 1919–1923. [[CrossRef](#)]
33. Chung, D.Y.; Jun, S.W.; Yoon, G.; Kim, H.; Yoo, J.M.; Lee, K.-S.; Kim, T.; Shin, H.; Sinha, A.K.; Kwon, S.G.; et al. Large-Scale Synthesis of Carbon-Shell-Coated FeP Nanoparticles for Robust Hydrogen Evolution Reaction Electrocatalyst. *J. Am. Chem. Soc.* **2017**, *139*, 6669–6674. [[CrossRef](#)] [[PubMed](#)]
34. Jing, S.Y.; Lu, J.J.; Yu, G.T.; Yin, S.B.; Luo, L.; Zhang, Z.S.; Ma, Y.F.; Chen, W.; Shen, P.K. Carbon-Encapsulated WO_x Hybrids as Efficient Catalysts for Hydrogen Evolution. *Adv. Mater.* **2018**, *30*, 1705979. [[CrossRef](#)] [[PubMed](#)]

